Available online at www.sciencedirect.com
SCIENCE DIRECT
Polymer 46 (2005) 10750–10757
polymer
www.elsevier.com/locate/polymer

Poly(ethylene oxide) and its blends with sodium alginate

Tuncer Çaykara[a,*], Serkan Demirci[a], Mehmet S. Eroğlu[b], Olgun Güven[c]

[a] Department of Chemistry, Faculty of Art and Science, Gazi University, 06500 Besevler, Ankara, Turkey
[b] Department of Chemical Engineering, Marmara University, 34722 Göztepe, Istanbul, Turkey
[c] Department of Chemistry, Hacettepe University, 06532 Beytepe, Ankara, Turkey

Received 1 February 2005; received in revised form 18 July 2005; accepted 2 September 2005
Available online 26 September 2005

Abstract

A series of blends based on poly(ethylene oxide) (PEO) and sodium alginate (NaAlg) were prepared by solution casting method. The blends thus obtained were characterized by using Fourier transform infrared spectroscopy (FT-IR), thermogravimetric analysis (TGA), differential scanning calorimetry (DSC), tensile strength test, contact angle measurements and atomic force microscopy (AFM). FT-IR studies indicate that there are the hydrogen bonding interactions due to the ether oxygen of PEO and the hydroxyl groups of NaAlg. The thermal stability of the blends was slightly affected with increasing NaAlg content. DSC results showed that both melting point and crystallinity depend on the composition of the blends. Mechanical properties of the blend films were improved compared to those of homopolymers. Surface free energy components of the blend films were calculated from contact angle data of various liquids by using Van Oss–Good methodology. It was found that the surfaces both of the blends are enriched in low surface free energy component, i.e. NaAlg. This conclusion was further confirmed by the AFM images observation of the surface morphology of these blends.

Keywords: Miscibility; Poly(ethylene oxide); Sodium alginate

1. Introduction

The importance of polymeric blends has been increased in recent years because of the preparation of the polymeric materials with desired properties, low basic cost, and improved processability. Polymeric blends are physical mixtures of structurally different polymers or copolymers which interact with secondary forces with no covalent bonding such as hydrogen bonding, dipole–dipole forces and charge-transfer complexes for homopolymer mixtures [1–4].

The blend materials from either synthetic or natural polymers alone are not always able to meet all the complex demands of the biomaterials. The success of synthetic polymers as biomaterials relies on their wide range of mechanical properties, transformation processes that allow a variety of different shapes to be easily obtained, and at low production cost. Biological polymers present good biocompatibility, but their mechanical properties are often poor. The necessity of preserving biological properties complicates their processability, and their production or recovery cost are very high [5]. Therefore, biologically polymeric important materials based on the blends of synthetic and natural polymers have been prepared, such as poly(*N*-vinyl-2-pyrrolidone)-kappa-carrageenan (PVP/KC), poly(*N*-vinyl-2-pyrrolidone)-iota-carrageenan (PVP/IC) [6], poly(ethylene oxide)-hydroxypropyl methylcellulose (PEO/HPMC) [7], poly(vinyl alcohol)-chitosan (PVA/C) [8].

Alginates, a naturally occurring polysaccharide obtained from marine brown algae, comprising linear chain of (1,4)-β-D-mannuronic acid and (1,3)-α-L-guluronic acid [9]. Sodium alginate (NaAlg), a polyelectrolyte having rigid molecular chain [10], and good film forming ability, has been extensively exploited and studied in detail on biomedical applications as a drug carrier [11,12].

Generally, the formation of specific intermolecular interactions through hydrogen bonding between two or more polymers is responsible for the observed mixing behaviors and properties of the blends prepared from aqueous solutions [13]. The study of the blends properties is of importance to explore further applications of the resulting blends for biomedical and pharmaceutical devices. Poly(ethylene oxide) [PEO] is a unique class of water-soluble, aerobically biodegradable thermoplastic [14,15]. Due to its excellent biocompatibility and very low toxicity, the potential use of PEO in biomedical

* Corresponding author.
E-mail address: caykara@gazi.edu.tr (T. Çaykara).

0032-3861/$ - see front matter © 2005 Elsevier Ltd. All rights reserved.
doi:10.1016/j.polymer.2005.09.041

applications has attracted a great deal of attention from both the industrial and scientific points of view [16–18]. Studies by Kondo et al. have established that the primary hydroxyl group on cellulose and methylcelluloses can form a hydrogen bond to ether oxygen in PEO [7]. Similarly, hydroxyl groups on sodium alginate can also form a hydrogen bond to the ether oxygen in PEO. So, PEO as a suitable candidate blended with NaAlg was therefore selected.

Theoretically, the miscibility of polymer blends is mainly determined by the chemical structure, composition and molecular mass of each component. In some cases, the preparation conditions of the blends are also decisive. Experimentally, various techniques have been used to characterize the miscibility of polymer blends, such as optical transparency, Fourier transform infrared spectroscopy (FT-IR), electron microscopy, differential scanning calorimetry (DSC), dynamic mechanical thermal analysis (DMTA) and high-resolution solid state ^{13}C nuclear magnetic resonance (NMR) [19,20]. Each technique bears intrinsic limitations in terms of sensitivity of detectable phase domain size. Therefore, the phase separation observed by one of these techniques cannot provide a perfect reflection of the thermodynamic definition of miscibility.

In this study, we focused on the binary blends of PEO and NaAlg to investigate their miscibility as a function of blend composition by the techniques of FT-IR, thermogravimetric analysis (TGA), DSC, mechanical testing, contact angle measurements and atomic force microscopy (AFM). Thereafter, the miscibility, intermolecular interactions and some fundamental morphological and structure property correlations in PEO/NaAlg blends are addressed.

2. Experimental

2.1. Materials

Sodium alginate (high viscosity) and poly(ethylene oxide) (MW = 300,000 g/mol) were obtained from Sigma Chemical Co. and Aldrich, respectively, and used as received.

2.2. Preparation of the films

Aqueous solutions of the individual polymers (1% w/v) were mixed to obtain the desired proportions and stirred for 30 min at room temperature. The pure and mixture solutions both transparent (wt% of NaAlg; 9, 20, 33, 43, 50) were cast on Petri dishes by water evaporation at 25 °C. The films were dried under vacuum at 60 °C for 10 days. The dried films of thickness ranging 40 ± 7 μm were obtained.

2.3. Fourier transform infrared spectroscopy (FT-IR)

FT-IR spectra of the blends were measured on a Nicolet 520 FT-IR spectrophotometer. The samples were prepared by making KBr (potassium bromide) pellets containing 3 wt% of materials.

2.4. Thermogravimetric analysis (TGA)

The dynamic weight loss tests were conducted on a TA instrument 2050 thermogravimetric analyzer (TGA). All tests were conducted in a N_2 purge (25 mL/min) using sample weights of 5–10 mg over a temperature range 20–600 °C at a scan rate of 10 °C/min.

2.5. Differential scanning calorimetry (DSC)

The glass transition temperatures of the blends were determined by use of a TA instrument DSC 2010 thermal analyzer system. DSC was calibrated with metallic indium (99.9% purity). All polymers were tested in crimped aluminum pans at a heating rate of 10 °C/min under dry N_2 gas (25 mL/min) over a temperature range from 20 to 175 °C. Melting temperature was taken as the peak of the melting endoterm. The error in each measurement was estimated to be ± 0.5 °C.

2.6. Mechanical measurements

The stress–strain measurements of the blends were performed by a AG-A electron tensiletester (Schimadzu Co.) in the environment of 22 °C by using a crosshead speed of 5 mm/min. The rectangular samples with dimensions at 25 mm × 10 mm × 40 ± 7 μm were analyzed at room temperature. At least three samples were used for all mechanical measurements.

2.7. Contact angle measurements

The contact angles of water, glycerol, ethylene glycol, formamide and paraffin drops on the polymer films were measured with a Model G-III Contact Angle Meter (Kernco Instrument Co. Inc., El Paso, TX, USA). The one-liquid method (air–liquid drop-polymer system) was used. All measured contact angles were the average of three measurements.

2.8. Atomic force microscopy measurements

The microscopic image of the blends was determined by an atomic force microscopy (AFM; Nanoscope IIIa, Digital Instruments, Santa Barbara, CA, USA) with a nanoprobe 200 μm in length and a pyramidal oxide-sharpened silicon nitride cantilever with a spring constant of 0.12 N/m. The opening angle of tip was 45°. The amplitudes used of the drive signal applied to the cantilever oscillation were in the between 0.5 and 2 V. The scan rates ranged from 0.8 to 1 Hz. Tapping mode of operation was used to eliminate shear forces that may damage the films and reduce the image resolution. Images (2×2 μm^2) were undertaken in air at 25 °C.

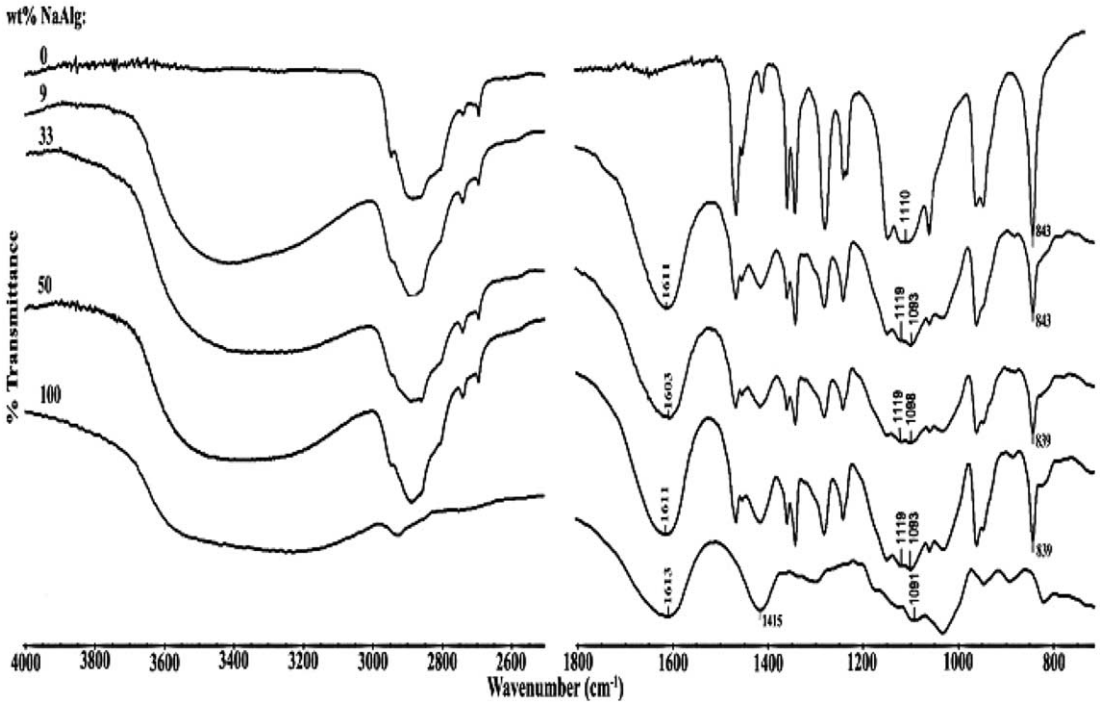

Fig. 1. The FT-IR spectra of the pure and blend films (4000–2500 and 1800–700 cm^{-1}).

3. Results and discussion

3.1. FT-IR

Fourier transform infrared (FT-IR) spectroscopy of blend films was carried out in order to detect any peak shift that could be attributed to weak interactions between the two polymers, such as hydrogen bonding or complexation. The FT-IR spectra of the interpolymer complexes show spectral features similar to those for the homopolymers, but the bands appear at shifted positions. Hydrogen bonds are formed between the proton-donor and proton-acceptor molecules. The intensity of the hydrogen bond band depends on the acidity of the hydrogen in the proton-donor, the alkalinity of the proton-acceptor and possibility of their close contacts. As a consequence of hydrogen bonding, the covalent bonds in the donor and acceptor are weaker, while the energy barrier for angle deformation becomes higher. Hence, in the groups which are involved in the hydrogen bonding formation, frequency of the valence vibrations decrease with the simultaneous increase in the frequency of the deformation vibrations.

Fig. 1 shows the FT-IR spectra of the pure and blend films in the wavelength ranges of 4000–2500 and 1800–700 cm^{-1}. The characteristic band of PEO was observed at 843 cm^{-1} due to the C–O–C bending. On the other hand, the bands of NaAlg appeared at 3500 cm^{-1} for the hydroxyl groups and at 1613 and 1415 cm^{-1} for the asymmetric $–COO^-$ stretching vibration and symmetric $–COO^-$ stretching vibration, respectively. The spectrum of the PEO/NaAlg blend films was characterized by the presence of the absorption bands typical of the pure components, with the intensity roughly proportional the blending ratio. The characteristic bands of NaAlg appeared at 1611 and 3500 cm^{-1} were observed in all spectra of the blends. The spectrum of the PEO/NaAlg blend films shows a significant difference in the region of the C–O–C asymmetric stretch at 1100 cm^{-1}. The blend films that have undergone the step transition show a broader C–O–C band compared with the pure components that have not. This broadening results in a band shift to lower wavenumber. The change in the C–O–C band in the spectrum, suggests that hydrogen bonding is the underlying mechanism in the interaction. In addition, hydrogen bonding has the strongest influence on the donor (in our case the –OH of NaAlg) and the absorption maxima of stretching vibration shifts toward lower wavenumbers compared to that for the pure NaAlg. It is also noticed that the hydroxyl stretching bands became much more broad with increasing NaAlg content. This strongly supports the idea that a hydrogen bonding can form between ether oxygen atoms of PEO and hydroxyl groups of NaAlg (Scheme 1).

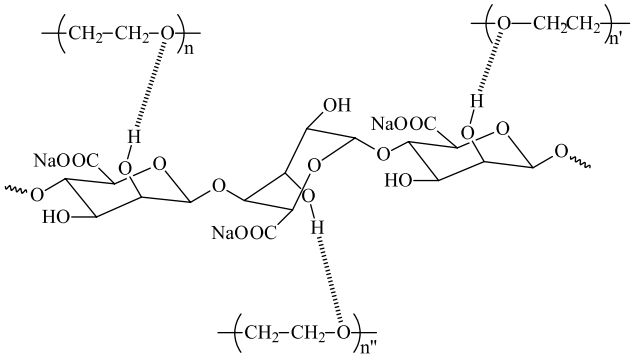

Scheme 1.

3.2. TGA

Typical weight loss (TG) and derivative of weight loss (DTG) curves of PEO, NaAlg and PEO/NaAlg blends were presented in Figs. 2 and 3. From the TG curves initial degradation temperature and final degradation temperature were determined. From DTG curves, the maximum temperature of weight loss was also noted.

The mass loss of pure PEO begins at 360 °C and reaches to maximum at 395 °C. However, the mass loss of pure NaAlg starts at 229 °C and reach to maximum at 243 °C. The PEO shows better thermal stability than that of NaAlg. The TG curves of both NaAlg and PEO also indicate one reaction stage (Fig. 2) which is reflected as single peak in the DTG curves (Fig. 3). However, PEO/NaAlg blends degrade in two steps. This is evidenced by the appearance of distinct peaks in DTG thermograms. Two distinct reaction peaks at around 240 and 408 °C are identified in the DTG thermograms of PEO/NaAlg blends. These peaks were attributed to thermal degradation of

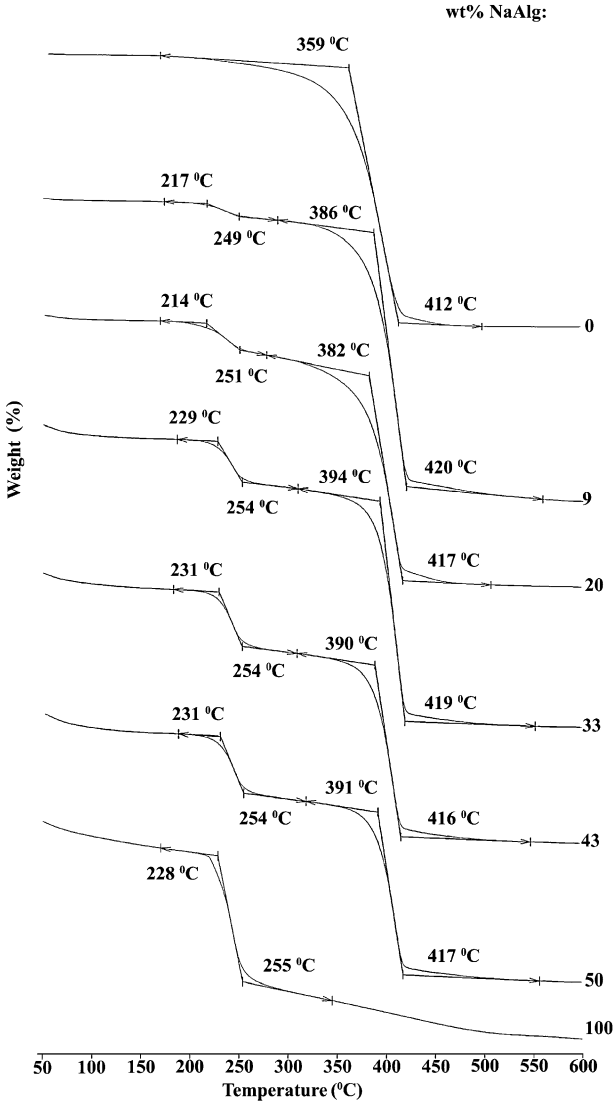

Fig. 2. The TGA curves of the pure and blend films.

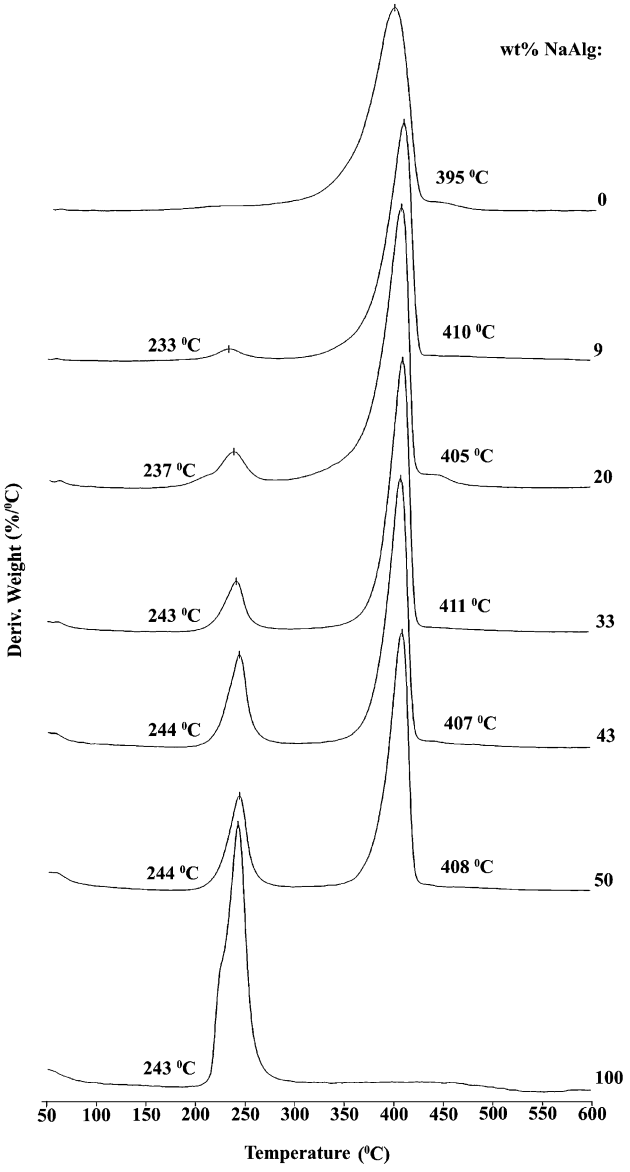

Fig. 3. The DTGA curves of the pure and blend films.

NaAlg and PEO, respectively. This behavior showed that the thermal degradation reaction mechanism of PEO/NaAlg blends is the same as pure PEO and NaAlg homopolymers. On the other hand, the initial thermal degradation temperatures of the blends were slightly affected with increasing NaAlg. This may be corresponded to the formation of hydrogen bonding from the ether oxygen of PEO and the hydroxyl groups of NaAlg in the PEO/NaAlg blends.

3.3. DSC

Fig. 4 shows the DSC curves of NaAlg, PEO and their blends. From these curves, crystallinity (X_c) of PEO in the blends was calculated by the following equation.

$$X_c = \frac{\Delta H}{f_w \Delta H_0} \quad (1)$$

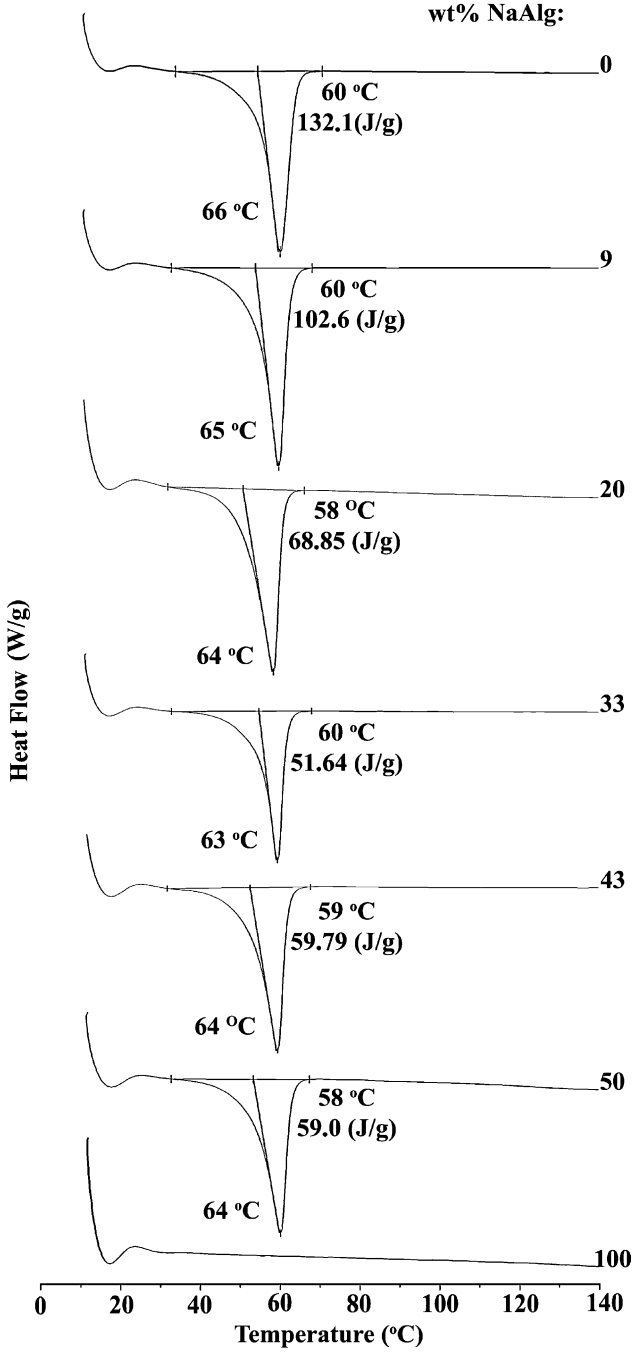

Fig. 4. The DSC curves of the pure and blend films.

where $\Delta H_0 = 18{,}810$ J/g is the heat of fusion for 100% crystalline PEO [21], ΔH is the heat of fusion of the blend and f_w is the weight fraction of PEO in the corresponding blend. The X_c and melting points (T_m) values were shown in Fig. 5. It was notable that both the T_m and X_c values decreased with increasing NaAlg content when NaAlg content is less than 33% and then increased. Both of these parameters have minimum values when the blend contains 33% NaAlg. The decrease of both the T_m and X_c values may be due to the stiff molecular chain of NaAlg, which has a significant effect on the overall chain mobility in the mixture and retards the rate of crystal growth.

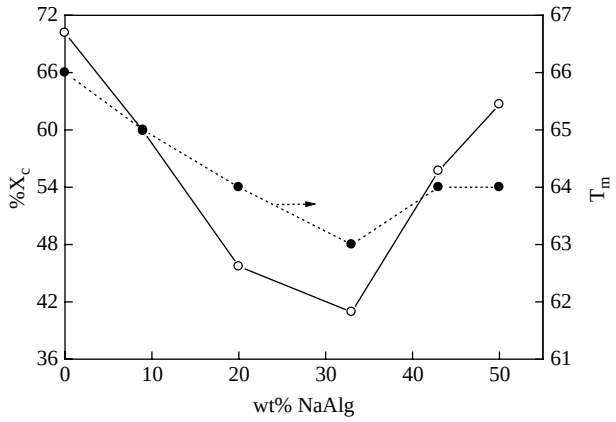

Fig. 5. The effect of the NaAlg content on melting point and crystallinity.

3.4. Mechanical properties

The results of the stress–strain measurements of NaAlg and PEO/NaAlg blend films were presented in Fig. 6. By casting from aqueous solutions, pure PEO rendered slightly opaque and brittle films and it was not possible to measure its mechanical properties. NaAlg, on the other hand, is a very strong material with a great stress and Young modulus. For the blends, the incorporation of NaAlg made the films stronger. The trend of the stress–strain values of the blend films is in good agreement with the results from FT-IR, TGA and DSC and hydrogen bonding is advantageous to improving the mechanical properties. When the mechanical properties of pure components were compared with their blends, it was observed that, the Young modulus and the stress and the elongation at break increased with increasing NaAlg content. This may be due to the intermolecular hydrogen bonding between NaAlg and PEO, such as those reported for the blend films of silk fibroin/NaAlg [22] and poly(acrylamide)/NaAlg [23].

3.5. Surface free energy analysis

Contact angles are characteristic constants of liquid–solid systems and provide valuable information on the surface energies of solids. The contact-angle values of paraffin oil, water, glycerol, ethylene glycol, formamide drops on the surface of PEO, NaAlg and their blend films with different

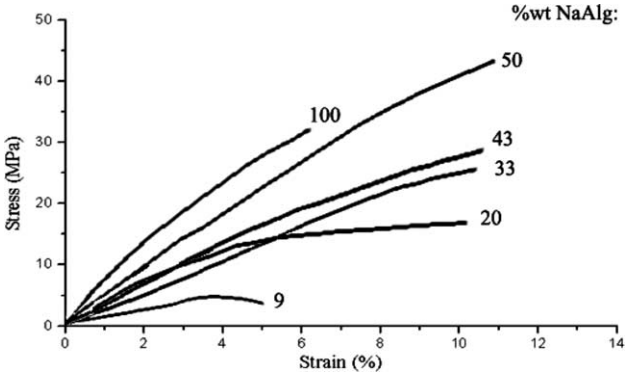

Fig. 6. Stress–strain curves of the pure and blend films.

Table 1
Contact angle results of PEO/NaAlg

NaAlg (wt%)	Paraffin	Water	Glycerol	Ethylene glycol	Formamide
0	10.0±0.0	48.0±0.4	50.0±0.0	35.0±0.0	60.0±0.0
9	20.8±0.4	52.8±0.4	53.7±0.5	35.9±0.7	47.8±0.8
20	25.0±0.5	57.0±0.0	60.9±0.9	38.2±0.4	43.0±0.6
33	29.0±0.6	62.3±0.5	65.9±0.4	39.1±0.6	34.3±0.5
43	34.0±0.0	66.2±0.4	70.0±0.0	45.0±0.0	30.0±0.0
50	39.2±0.8	70.0±0.0	74.0±0.6	47.1±0.7	27.8±0.4
100	46.1±0.4	78.0±0.5	68.0±0.8	47.2±0.4	25.0±0.6

NaAlg content are shown in Table 1. The surface free energy components of these blend films containing various weight percentage of NaAlg were determined from the contact angle data of polar and apolar liquids by using the following complete Young equation comprising both the apolar and polar interactions [24,25]

$$\gamma_L(1+\cos\theta) = 2\left(\sqrt{\gamma_s^{LW}\gamma_s^{LW}} + \sqrt{\gamma_s^-\gamma_s^+} + \sqrt{\gamma_s^+\gamma_s^-}\right) \quad (2)$$

In the above equation, the superscript LW represents the apolar Lifshitz–Van der Waals forces. Subscripts L and S refer to liquid and solid, respectively. γ_L is the total surface free energy of the liquid, θ is the contact angle of liquid drop on the solid surface, and γ_L^{LW} and γ_s^{LW} are the apolar Lifshitz–Van der Waals components of liquid and solid, respectively. γ_s^+ and γ_L^+ are the electron acceptor surface free energy components of solid and liquid, respectively. γ_s^- and γ_L^- are the electron donor surface free energy components of solid and liquid, respectively. γ_L^{LW} can be determined first by using an apolar liquid (paraffin). For an apolar liquid, $\gamma_L^+ = \gamma_L^- = 0$ and $\gamma_L^{LW} = \gamma_L$ hence, the last two terms of the right hand side of Eq. (1) become zero, this equation can therefore be written in the form

$$\gamma_s^{LW} = \frac{\gamma_L(1+\cos\theta)^2}{4} \quad (3)$$

Consequently, the γ_s^{LW} value can be determined directly from apolar liquid (paraffin) contact angle. When two polar liquids are used, two equations of the form of Eq. (1) constitute a set of two simultaneous equations which can be solved for the two unknown properties of solid γ_s^- and γ_s^+. Then the γ_s^- and γ_s^+ results are averaged for a single value. Water drop contact-angle values are always used in these sets in order to avoid large discrepancies between simultaneous equation solutions [26].

Table 2
Surface free energy component values of the liquids used [18] (mJ/m^2)

Liquid	γ_L^{TOT}	γ_L^{LW}	γ_L^+	γ_L^-
Paraffin	28.9	28.9	0	0
Water	72.8	21.8	25.5	25.5
Glycerol	64.0	34.0	3.92	57.4
Ethylene glycol	48.0	29.0	1.92	47.0
Formamide	58.0	39.0	2.28	39.6

Table 3
Surface free energy components of PEO/NaAlg blend films (mJ/m^2)

NaAlg (wt%)	γ_s^{LW}	γ_s^+	γ_s^-	γ_s^{TOT}
0	28.46	1.37	40.99	80.26
9	27.05	1.49	30.72	78.52
20	26.26	1.81	26.14	75.59
33	25.29	3.09	19.38	72.74
43	24.17	3.91	16.49	69.70
50	22.76	4.85	13.76	66.83
100	20.72	7.71	5.40	63.48

The contact-angle values of the liquids used were evaluated to determine the surface free energy components of PEO/NaAlg blend films with various NaAlg content by using Van Oss–Good methodology thorough Eqs. (1) and (2). The surface free energy component values of the liquids used were taken from Ref. [26] and given in Table 2.

The LW component of the surface free energy of the blend films were calculated by using Eq. (2) and the paraffin oil drop contact-angle values and given in Table 3. As seen in this table, the γ_s^{LW} values of the blend films decreased with increasing NaAlg content. This can be explained on the basis that the NaAlg units of the blends have a higher dispersion force than that of the PEO units. It is well known that there is an inverse relationship between intermolecular distance and the dispersion forces present.

γ_s^+ and γ_s^- values of these blends were calculated using the general contact-angle equation (Eq. (1)), where previously found γ_s^{LW} values were inserted. Water–glycerol, water–ethylene glycol, and water–formamide sets were simultaneously solved and the average results were also given in Table 3. As shown in this table, the PEO has a highly basic character ($\gamma_s^- = 40.99$ mJ/m^2 > $\gamma_s^+ = 1.37$ mJ/m^2), whereas surface of the NaAlg has a slightly acidic character

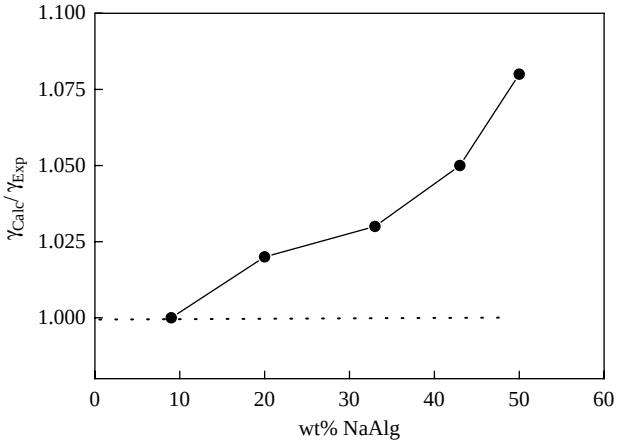

Fig. 7. The change of $\gamma_{Calc}/\gamma_{Exp}$ ratios of the blends with wt% NaAlg.

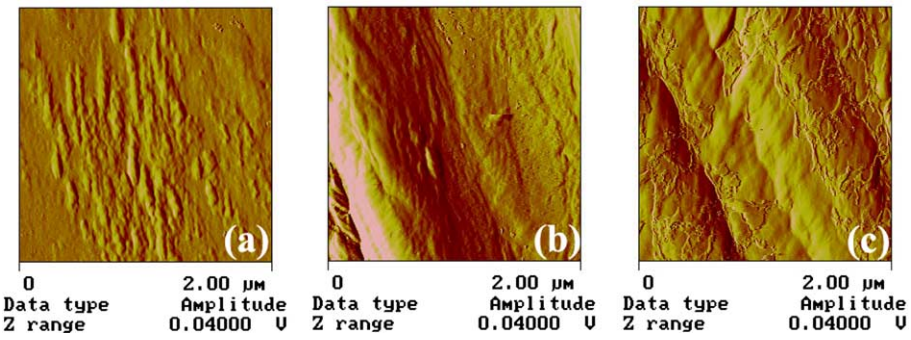

Fig. 8. AFM images of (a) pure PEO, (b) PEO/NaAlg (9 wt% NaAlg), (c) PEO/NaAlg (50 wt% NaAlg).

($\gamma_s^+ = 7.71$ mJ/m$^2 > \gamma_s^- = 5.40$ mJ/m^2). Generally, the PEO/NaAlg blends have also a highly basic character and the γ_s^- values decreased with increasing NaAg in the blends. The decrease of both $\gamma_s^{LW}$and γ_s^- values also reflected in the decrease of total surface energy (γ_s^{TOT}) of the blends with increasing NaAlg content. In addition, the PEO has a higher γ_s^{TOT} value than that of NaAlg (Table 3). Thus, it is the reason for NaAlg enhanced on the surface of all blend systems. It is well known that some surface enrichment of the low surface free energy component takes place in the blend systems [27].

We have also tried to calculate the total surface free energy (γ_s^{TOT}) of the blends from the following equation, assuming additivity rule;

$$\gamma_s^{TOT}(\text{Blend}) = \phi_1 \gamma_s^{TOT}(1) + \phi_2 \gamma_s^{TOT}(2) \quad (4)$$

where ϕ_1 and ϕ_2 denote the weight percentage of PEO and NaAlg in the blend, $\gamma_s^{TOT}(1)$ and $\gamma_s^{TOT}(2)$ are the total surface energies of pure PEO and NaAlg, respectively. The ratios of the calculated total surface energy values to the experimental total surface energy values ($\gamma_{Calc}/\gamma_{Exp}$) increased with increasing NaAlg in the blend, which is plotted in Fig. 7. As shown in this figure, the $\gamma_{Calc}/\gamma_{Exp}$ values of these blends are always higher than 1. This is mainly due to increasing of the component with the low surface free energy of blends at the surface.

3.6. AFM

The AFM images of PEO and PEO/NaAlg films are shown in Fig. 8. The surface morphology characteristics of PEO film and its blends with NaAlg are observed to depend on composition. As shown in Fig. 8, the PEO film has relatively uniform surface structure, while its blends with NaAlg start to show two separated phases. This observation agrees very well with the contact angle observations. Although the micro-separation could not be observed for low NaAlg containing blends, the separation becomes more evident at 50% mixtures. The boundary between two phases developed with increasing concentrations of NaAlg and at 50% composition small islands of NaAlg formed at the surface. This is in good agreement with the results obtained by contact angle measurements, where an enrichment of NaAlg on the blend surface was observed.

4. Conclusions

Blend films of PEO and NaAlg could be easily obtained over the whole composition range from water solutions by solution blending and casting onto the glass plate. Mechanical properties of the blends were enhanced relative to those of PEO and NaAlg. The enhancement is caused by the existence of specific intermolecular interactions between PEO and NaAlg in the blend. FT-IR analysis revealed this interaction from the shift and change of intensity of –OH and C–O–C bands. The thermal stability of the blends was slightly affected depending on NaAlg component. NaAlg was found to hinder the crystallization of PEO during casting, and to reduce the stability (i.e. melting temperature) of crystals. The results of AFM showed microscopic phase separation and islands on the surfaces of the blends because of the aggregation of NaAlg content. The phase separation increased with an increase of NaAlg content. The surface free energy of blends decreased with increasing NaAlg component to a considerable extent. It was determined that the casting from water solutions had an effect on localizing the remaining blend compositions on the surface of the films different from the bulk composition. Both, contact angle measurements and AFM investigations have proved that the surface of the blends is enriched in NaAlg component.

Acknowledgements

O.G. acknowledges the support of TÜBA, the Academy of Sciences of Turkey. The authors thank to Dr M.M. Demir from Sabancı University for AFM measurements. This work was supported by State Planning Organization of Turkey (2003 K 120 470-31 DPT).

References

[1] Krause S. Polymer blends. New York: Academic Press; 1979.
[2] Varnell DF, Coleman MM. Polymer 1981;22:1324.
[3] Varnell DF, Runt JP, Coleman MM. Polymer 1983;24:37.
[4] Woo EM, Barlow JW, Paul DR. J Appl Polym Sci 1986;32:3889.
[5] Maria GC. Polym Int 1997;43:55.
[6] Relleve L, Yoshii F, Rosa DA, Kume T. Angew Makromol Chem 1999; 273:63.
[7] Kondo T, Sawatari C. Polymer 1994;35(20):4423.
[8] Miya M, Iwamoto R. J Polym Sci, Part B: Polym Phys 1984;22:1149.

[9] Moe ST, Skjak-brek G, Ichijo H. J Appl Polym Sci 1994;51:1773.
[10] Hirano S, Mizutani C, Yamaguchi K, Miura O. Biopolymers 1978;17: 805.
[11] Yuk SH, Cho SH, Lee HB. J Controlled Release 1995;7:69.
[12] Hari PR, Chandy T, Sharma CP. J Appl Polym Sci 1996;59:1795.
[13] Sun Y, Shao Z, Hu P, Liu Y, Yu T. J Polym Sci, Part B: Polym Phys 1997; 35:1405.
[14] Bailey FE, Koleske JV. Poly(ethylene oxide). New York: Academic Press; 1976.
[15] Ramachandran R. Plast Eng 1996;52:31.
[16] Desai NP, Hubbell JA. Biomaterials 1991;12:144.
[17] Desai NP, Hubbell JA. Macromolecules 1992;25:226.
[18] Lee JH, Kopecek J, Andrade JD. J Biomed Mater Res 1989;23:351.
[19] Cowie JMG. Encylopedia of polymer science and engineering. New York: Wiley; 1989.
[20] Walsh DJ. Comprehensive polymer science. New York: Pergamon Press; 1989.
[21] Kim KM, Chiou JS, Barlow JW, Paul DR. Polymer 1987;28:1721.
[22] Liang CX, Hirabayashi K. J Appl Polym Sci 1992;45:1937.
[23] Xiao C, Lu Y, Liu H, Zhang L. J Macromol Sci Pure Appl Chem 2000;37: 1663.
[24] Van Oss CJ, Good RJ. Langmuir 1992;8:2877.
[25] Erbil HY. Langmuir 1994;10:276.
[26] Van Oss CJ. Interfacial forces in aqueous media. New York: Marcel Dekker; 1994.
[27] Çaykara T, Eroğlu MS, Güven O. J Appl Polym Sci 1998;69:1551.